Generation of Numerical Data for the Facilitation of the Personalized Hyperthermic Treatment of Cancer with an Interstitial Antenna Array Using the Method of Symmetrical Components

Prodromos E. Atlamazoglou
Greek Ministry of Defense

The method of moments combined with the method of symmetrical components is used for the analysis of interstitial hyperthermia applicators. The basis and testing functions are both piecewise sinusoids, qualifying our technique as a Galerkin one. The dielectric coatings are modeled by equivalent volume polarization currents, which are simply related to the conduction current distribution, avoiding in that way the introduction of additional unknowns or numerical integrations. The results of our method for a four-dipole circular array, are in agreement with those already published in literature for a same hyperthermia configuration. Apart from being accurate, our approach is more general, more computationally efficient and takes into account the coupling between the antennas.

INTRODUCTION

Hyperthermia is the use of heat for the destruction of malignant tissues, in the treatment of cancer (Hahn, 1982). One of the most efficient ways to heat a tumor is by illuminating it with microwaves. Tumor temperatures above $42 - 43^{o}$C for a sufficient period of time, have been proven deadly for its cells. As heating can be also dangerous for the healthy tissues surrounding the tumor, those must be kept at significantly lower temperatures. This can prove a significant challenge in the design of personalized hyperthermia treatment protocols. In clinical practice hyperthermia is used as an adjutant to both chemotherapy and radiation therapy, since it can enhance their therapeutic efficiencies.

Noninvasive techniques for administering microwave hyperthermia offer certain clinical advantages, but at the cost of great difficulty in the control of the heating patterns. As a solution to this problem Mendecki *et al* and Taylor (Mendecki *et al*, 1977; Taylor, 1978), first suggested in 1977 and 1978 respectively, the use of interstitial microwave antennas, inserted directly into the tumor. These antennas are insulated dipoles, and they are implanted into the treated tissue via catheters often already *in situ* for the application of brachytherapy.

The field radiated by a single dipole embedded in a tumor, has been shown to decay rapidly with distance (King, Trembly & Strobhen, 1983). This is due to the highly dissipative nature of the surrounding medium. The result is a limited heating effect, concentrated to a small volume around the antenna. As this is clearly unsatisfactory, in practice interstitial antennas are used in arrays of two or more dipoles positioned around the treated tumor. Apart from the larger heated volume, the use of arrays offers

greater flexibility in controlling the patterns of energy distribution, by adjusting the characteristics of the individual antenna elements, their relative positions and their excitation.

Due to the shortage of widely available experimental data of the electric field and the temperature distributions inside the tumors during the application of hyperthermia treatment, approximate and computational techniques have been developed for the generation of numerical data. Many distinguished researchers have studied interstitial antennas and their arrays in the context of hyperthermia. Two models have been proposed for their simulation. The first put forward by King *et al.*, treats each interstitial antenna as a symmetric dipole. This model is relatively simple, and yields results that agree with experimental measurements in lateral planes near the antenna tip. However, the symmetrical dipole hypothesis has not been validated along the axis of the antenna.

An alternative model is that introduced by Zhang *et al* (Zhang, Dubal & Takemoto-Hambleton, 1988). This second model views an interstitial antenna as an asymmetric dipole with two arms of unequal length. The length of the shorter arm is equal to the halflength of the symmetric model, while the size of the other arm is determined experimentally. The concept of this model is intuitively justified by the actual interstitial antenna's physical asymmetry about the radiation gap along its axis. But this model is also successful from the point of experimental validation. It leads to results that are in good agreement with experiments in the lateral as well as the axial plane.

Both of the above models can only be applied when the complex permittivity of the ambient medium is much greater than that of the insulating layer, which is considered to extend to infinity. In (Atlamazoglou & Uzunoglou, 1998) we proposed a Galerkin moment method for the analysis of a single coated dipole in a lossy medium, that is not subject to these restrictions, and at the same time is considerably more efficient for field computations. That method has been widely accepted by the scientific community as it has been adopted in various areas of application ranging from MRI safety (Yeung, Susil & Atalar, 2001), (Yeung *et al*, 2002), (Park, Kamondetdacha, Amjad & Nyebhuis, 2005), (Mohsin, Sheikh, U. Saeed, 2008), (Mohsin *et al, 2008*) and the safety of implanted cardiac pacemakers (Jakobus, Ruos, Geisbush & Landstorfer, 1999) to Geophysical and Remote Sensing Applications (Liu & Sato, 2005), (Ebihara & Hashimoto, 2005) and even the analysis of railway grounding systems subjected to lightning strikes (Jacqmaer, Geuzaine & Driesen, 2008).

The purpose of the presented work is the extension of (Atlamazoglou *et al*, 1998) to arrays of insulated antennas.

For those not familiar with our previous work in (Atlamazoglou *et al*, 1998), the following section contains a brief overview of it. The third section describes the method of symmetrical components, and its application for the analysis of interstitial antenna arrays. The last two sections discuss the numerical results of the method for a four-antenna circular array and provide the necessary conclusions.

In the following analysis, a time dependence $e^{j\omega t}$ is assumed and suppressed for all sources and fields.

SINGLE ANTENNA ANALYSIS

FIGURE 1
AN INSULATED DIPOLE

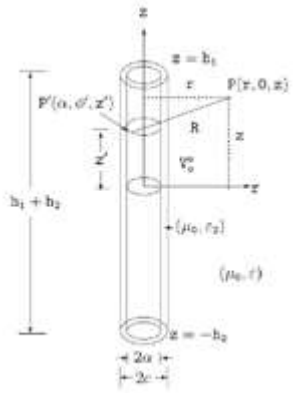

By making the well-known thin-wire approximations, the reaction integral equation for a bare cylindrical antenna takes the form

$$\frac{j\omega\mu_0}{8\pi^2}\int_{-h_2}^{h_1}\int_{-\pi}^{\pi}\left(\int_{-h_2}^{h_1}\int_{-\pi}^{\pi}\left(1+\frac{1}{k^2}\frac{\partial^2}{\partial z^2}\right)\frac{e^{-jkR}}{R}\right.$$

$$I_t(z')d\phi' dz')I_S(z)d\phi dz = V_o{}^e I_t(0) \tag{1}$$

where

$$R=\sqrt{(z-z')^2+4\alpha^2\sin^2\left(\frac{\phi-\phi'}{2}\right)}. \tag{2}$$

This equation can be solved via a Galerkin moment method that uses piecewise sinusoids as expansion and testing functions. Piecewise sinusoids are subdomain functions defined by

$$F_n(z)=\begin{cases}\frac{\sin\left(k(z-z_{n-1})\right)}{\sin\left(k\Delta z\right)}, & z_{n-1}\le z\le z_n\\ \frac{\sin\left(k(z_{n+1}-z)\right)}{\sin\left(k\Delta z\right)}, & z_n\le z\le z_{n+1}\\ 0, & elsewhere\end{cases} \tag{3}$$

where $\Delta z = z_n - z_{n-1} = z_{n+1} - z_n$. By substituting $I_S(z)$ in (1) by an expansion of it in terms of piecewise sinusoids with unknown coefficients and enforcing the integral equations for N distinct test sources F_n, a linear system equations is obtained. Because of the similarity of the basis functions and testing functions selected (they all have the same orientation and equal support), all the elements of every diagonal of the system's coefficient matrix are identical to each other. This means that the system is a symmetric Toeplitz one, and the very fast Levinson's method (Press, Flannery, Teukolsky & Vetterling, 1989) can be used its solution.

Each element Z_{mn} of the coefficient matrix of the system is given by the expression

$$Z_{mn} = \frac{j\omega\mu_0}{4\pi k \sin^2(k\Delta z)} \int_{z_{m-1}}^{z_{m+1}} \int_{-\pi}^{\pi} \left(\frac{e^{-jkR_{n+1}}}{R_{n+1}} \right.$$

$$\left. + \frac{e^{-jkR_{n-1}}}{R_{n-1}} - 2\cos(k\Delta z) \frac{e^{-jkR_n}}{R_n} \right)$$

$$\cdot \sin(k(\Delta z - |z' - z_m|)) d\phi' dz' \tag{4}$$

where

$$R_l = \sqrt{(z' - z_l)^2 + 4\alpha^2 \sin^2\left(\frac{\phi'}{2}\right)},$$

$$l = n+1, n-1, n. \tag{5}$$

The double integration in (4), must be performed numerically. The integrand is characterized by singularities at $\phi' = \phi$, $z' = z_{n+1}$, z_{n-1}, and z_n. Although these singularities are integrable, it is preferable to subtract them, in order to perform the integrations more efficiently. The isolated singular terms can be shown to be complete elliptic integral of the first kind, for which a polynomial approximation algorithm can be used for its computation.

The above formulation can be extended to take into account the dielectric coating of an insulated dipole. Using the volume equivalence theorem, this coating can be replaced with ambient medium and an equivalent volume polarization current

$$\boldsymbol{J}_P = j\omega(\varepsilon_2 - \varepsilon)\boldsymbol{E} \tag{6}$$

where **E** is the electric field inside the coating, and ε_2 and ε denote the permittivities of the insulation and the ambient medium respectively.

Because of this new additional current $\boldsymbol{J}_P$, the reaction integral equation becomes for the case of a coated dipole

$$\int\int_S E_{tz} J_{Sz} dS + \int\int\int_V E_{tr} J_{Pr} dV = \int\int_S E_{Sz} J_{tz} dS. \tag{7}$$

Ordinarily E_{tr} and J_{Pr}, in the area of the dielectric coating are unknown functions. But as the insulating layer is thin, these quantities can be expressed approximately as functions of J_{Sz}. By using Maxwell's equations and quasistatic approximations to them, we derive the following approximate expressions

$$E_r(r,z) = \frac{j}{\omega 2\pi r \varepsilon_2} \frac{dI_S(z)}{dz}. \tag{8}$$

$$\boldsymbol{J}_P(r,z) = \frac{(\varepsilon - \varepsilon_2)}{2\pi\varepsilon_2 r} \frac{dI_S(z)}{dz} \tag{9}$$

Therefore, any new unknowns associated with the polarization current, are dependent upon the original ones, and this relation keeps the total number of unknowns the same as that for the bare dipole

analysis. Naturally, some of the elements of the moment-method matrix are modified. The analysis that determines these modifications is described in detail in (Atlamazoglou *et al.,* 1998).

The main points of that analysis can be summarized as follows. Each basis function used for the expansion of the conduction current is related to a part of the radial volume polarization current. Therefore, each element of the moment method matrix Z_{mn} for an insulated antenna, has an additional term. These terms can be thought of as forming a new matrix ΔZ, that when added to the moment method matrix for a bare antenna, gives the coated dipole's matrix.

If piecewise sinusoids are used as basis and testing functions, ΔZ turns out to be symmetric, tridiagonal and Toeplitz. Its elements are given by the relations

$$\Delta Z_{n,n} = \frac{jk}{2\pi\omega}\frac{(\varepsilon-\varepsilon_2)}{\varepsilon\varepsilon_2}\ln\left(\frac{c}{\alpha}\right)\left(\frac{k\Delta z}{sin^2(k\Delta z)}+\frac{1}{tan\,(k\Delta z)}\right) \tag{10}$$

$$\Delta Z_{n,n-1} = \frac{-jk}{4\pi\omega\, sin\,(k\Delta z)}\frac{(\varepsilon-\varepsilon_2)}{\varepsilon\varepsilon_2}\ln\left(\frac{c}{\alpha}\right)\left(1+\frac{k\Delta z}{tan\,(k\Delta z)}\right) \tag{11}$$

$$\Delta Z_{n-1,n} = \Delta Z_{n,n-1} \tag{12}$$

As no numerical integrations are involved in the evaluation of ΔZ, it is obvious that the computational cost required for the construction of the moment method matrix for an insulated antenna, is practically equal to that for a bare antenna.

Due to rotational symmetry, the electric field radiated by the antenna in the ambient medium has only z and r components, that are independent of ϕ. The field at any point can be expressed as the superposition of the partial fields radiated by the expansion function currents, with weights the coefficients determined via the moment method.

The z component of the n expansion function's electric field is given by

$$E_{zn}(r,z) = -\frac{jk}{8\pi^2\omega\varepsilon\, sin\,(k\Delta z)}\int_{-\pi}^{\pi}\left(\frac{e^{-jkR_{n+1}}}{R_{n+1}}\right.$$

$$\left.+\frac{e^{-jkR_{n-1}}}{R_{n-1}}-2\cos(k\Delta z)\frac{e^{-jkR_n}}{R_n}\right)d\phi' \tag{13}$$

where

$$R_l = \sqrt{(z-z_l)^2+r^2+\alpha^2-2r\alpha\cos(\phi')},$$

$$l = n+1, n-1, n. \tag{14}$$

The corresponding formula for the radial field is

$$E_{rn}(r,z) = \frac{jk}{8\pi^2\omega\varepsilon\, sin\,(k\Delta z)}\int_{-\pi}^{\pi}\frac{r-\alpha\, cos\,(\phi')}{r^2+\alpha^2-2r\alpha\, cos\,(\phi')}$$

$$\cdot\left(\frac{e^{-jkR_{n+1}}}{R_{n+1}}(z-z_{n+1})+\frac{e^{-jkR_{n-1}}}{R_{n-1}}(z-z_{n-1})\right.$$

$$\left.-2\cos(k\Delta z)\frac{e^{-jkR_n}}{R_n}\right)(z-z_n))d\phi'. \tag{15}$$

The detailed derivation of the above relations is given in (Atlamazoglou *et al*, 1998). The numerical integrations in (13) and (15), can be performed by means of an adaptive quadrature routine based on the Gauss Kronrod rules.

For points not close to the surface of the insulation the following approximate versions of (13) and (15), can be used

$$E_{zn}(r,z) \doteq -\frac{jk}{4\pi\omega\varepsilon\, sin\,(k\Delta z)}\left(\frac{e^{-jkR'_{n+1}}}{R'_{n+1}}\right.$$

$$\left.+\frac{e^{-jkR'_{n-1}}}{R'_{n-1}} - 2\cos(k\Delta z)\frac{e^{-jkR'_n}}{R'_n}\right) \tag{16}$$

$$E_{rn}(r,z) \doteq \frac{jk}{4\pi\omega\varepsilon r\, sin\,(k\Delta z)}\left(\frac{e^{-jkR'_{n+1}}}{R'_{n+1}}(z-z_{n+1})\right.$$

$$+\frac{e^{-jkR'_{n-1}}}{R'_{n-1}}(z-z_{n-1})$$

$$\left.-2\cos(k\Delta z)\frac{e^{-jkR'_n}}{R'_n}(z-z_n)\right) \tag{17}$$

where

$$R'_l = \sqrt{(z-z_l)^2+r^2}, l = n+1, n-1, n. \tag{18}$$

The results obtained with (17) show excellent agreement with those from (15), for almost all values of r. However, the use of (16) leads to accurate results only in the relatively far region.
The electric field radiated in the ambient medium by the volume polarization current is neglected, as it is almost two orders of magnitude smaller than the conduction current's contribution.

FIGURE 2
A TYPICAL ARRAY OF PARALLEL COATED ANTENNAS

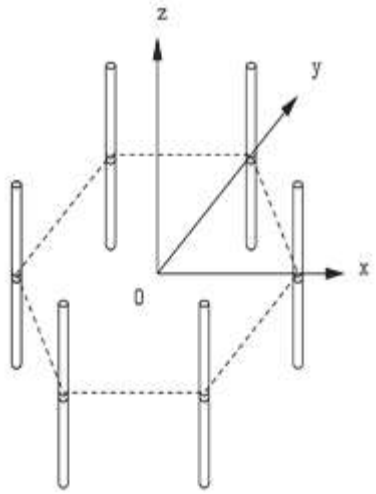

ANALYSIS OF CIRCULAR ARRAYS OF INTERSTITIAL ANTENNAS

The following analysis is restricted to the case of parallel antenna arrays. The reason for this is that arrays for interstitial hyperthermia, is almost exclusively of this form. Furthermore because of this assumption, the analysis is significantly simplified and as a consequence the computational cost of its implementation can be kept at low levels. However, the method of moments is general enough, so that it can be applied to arrays of arbitrary oriented antennas, but at the cost of a higher computational complexity.

Fig. 2 illustrates a typical array of parallel insulated dipoles. If the coordinates of their excitation gaps are (x_{oi}, y_{oi}, z_{oi}), where $i = 1,2, \dots, N$, and θ_i denote the time phase angles of the fields at each antenna, then the components of the total electric field at point (x, y, z) are given by the relations

$$E_x = \sum_{i=1}^{N} \frac{x - x_{0i}}{R_i} E_{ri} e^{j\theta_i} \tag{19}$$

$$E_y = \sum_{i=1}^{N} \frac{y - y_{0i}}{R_i} E_{ri} e^{j\theta_i} \tag{20}$$

$$E_z = \sum_{i=1}^{N} E_{zi}\, e^{j\theta_i} \tag{21}$$

where

$$R_i = \sqrt{(x - x_{0i})^2 + (y - y_{0i})^2}. \tag{22}$$

In order to compute the E_{ri} and E_{zi} for each antenna, its current distribution must be determined. The simplest way to do this is to make the assumption that the function of each antenna is not affected by the presence of the rest. This is the way that the analysis of interstitial hyperthermia arrays is carried out, in almost every other publication of the literature. The hypothesis of negligible coupling between the antennas of the array, is in the majority of the cases justified by the radiated field in the surrounding space, due to the high conductivity of the ambient medium. Having made this assumption, the integral equation for each dipole can be solved independently from the rest.

But in reality there exists coupling between the dipoles, even though it is indeed extremely weak. For our solutions to have increased accuracy, its effect must be included to the analysis. This can be done by solving simultaneously the N coupled integral equations for the antennas of an array. In every dipole's integral equation terms must be included, that express the fields of the other elements of the array on its conducting surface. It is assumed that the coating of the antennas does not affect these terms. The implementation of the method of moments for the solution of these integral equations, leads to a linear system of equations with unknowns the coefficients of the basis functions for all the antennas. This system is usually large even for small arrays, and as a result its solution is computationally intensive.

Both approaches described above, can be applied also to cases of arrays with non-parallel elements. But if the dipoles of an array are not only parallel but identical to each other and equally distributed in the circumference of an imaginary circle, then their array is called a circular one. In practice this kind of array is the one used more than any other, in applications of interstitial hyperthermia.

A circular antenna array can be analyzed very efficiently, by employing the method of symmetrical components (King, 1990). The first stage of the application of that method consists, in the determination of the current distribution of the antennas, when they are driven by the phase sequence voltages. These voltages are given the relation

$$V_i^{(m)} = V_1^{(m)} e^{j2\pi(i-1)m/N}, \quad \begin{cases} i = 1,2, \dots, N \\ m = 0,1, \dots, N-1 \end{cases} \tag{23}$$

where i and m are the indices of the antenna and the phase sequence respectively.
For every phase sequence m, $V_1^{(m)}$ is determined as a function of the N individual driving voltages V_i, by using the formula

$$V_1^{(m)} = N^{-1} \sum_{i=1}^{N} e^{-j2\pi(i-1)m/N} V_i. \quad (24)$$

The uniform characteristics of the elements of a circular array, combined with the pattern of the phase sequence voltages, have as a result the responses of the antennas to these excitations, the so-called phase sequence currents to differ from element to element, only a constant phase. This phase change is characteristic for each sequence.

$$I_i^{(m)}(z') = I_1^{(m)}(z') e^{j2\pi(i-1)m/N}. \quad (25)$$

This means that for each phase sequence, only the solution of the integral equation of a single antenna is required. By using (25), in the terms that express the effect of the other dipoles on it, the only unknown in that equation is the current distribution of the antenna associated with it. As soon as this unknown is determined, by solving the integral equation, it is fairly simple, again with the use of (25), to find out the current distributions of the remaining antennas for the same phase sequence.

It can be easily proved, that for every antenna the sum of its current distributions for all the phase sequences $I_i^{(m)}$, is equal to the response I_i to the true excitation voltages.

$$I_i(z') = \sum_{m=0}^{N-1} I_i^{(m)}(z') = \sum_{m=0}^{N-1} e^{\frac{j2\pi(i-1)m}{N}} I_1^{(m)}(z'). \quad (26)$$

It is obvious that for the analysis of a circular array with the method of symmetrical components, N independent integral equations have to be solved one for each phase sequence. By using this method, the coupling between the antennas is included in the analysis, while the computational cost for the solution of the arising linear systems is kept at low levels.

NUMERICAL RESULTS AND DISCUSSION

FIGURE 3
A CIRCULAR ARRAY OF FOUR INSULATED ANTENNAS

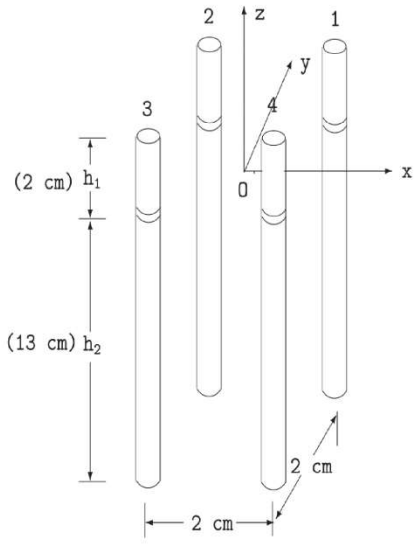

Fig. 3 shows the circular array that is used to investigate the accuracy and numerical efficiency of the method proposed in the previous sections. The array consists of four insulated asymmetric dipoles, positioned at the corners of a 2 cm edge square. The dipoles are identical, their axes parallel, and their excitation gaps are all at the $z = 0$ level. The radius of each antenna is $\alpha = 0.475$ mm, and its two arms have lengths $h_1 = 1.989$ cm and $h_3 = 13.0$ cm respectively. The catheters, inside which the dipoles are placed, are made of polypropylene and have inner radius $b = 0.584$ mm, outer $c = 0.805$ mm and relative permittivity$\varepsilon_{3r} = 2.55$. The ambient medium is muscle equivalent tissue and has relative permittivity $\varepsilon_{4r} = 51.0$ at 915 MHz, the operation frequency of the antennas. Its density is 970 Kg/m^3 and its conductivity $\sigma_4 = 1.28$ S/m.

The array described above has been analyzed repeatedly in literature (Zhang *et al*, 1990), (Clibbon, McCowen &Hand, 1993), by using other techniques as well as experimental measurements. This fact combined with the array's popularity in hyperthermia practice, led its choice as a test problem for our approach, for comparison and validation purposes.

FIGURE 4
MAGNITUDE OF THE COMPLEX CURRENT DISTRIBUTION OF ANTENNA, FOR ZERO PHASE SEQUENCE (m = 0)

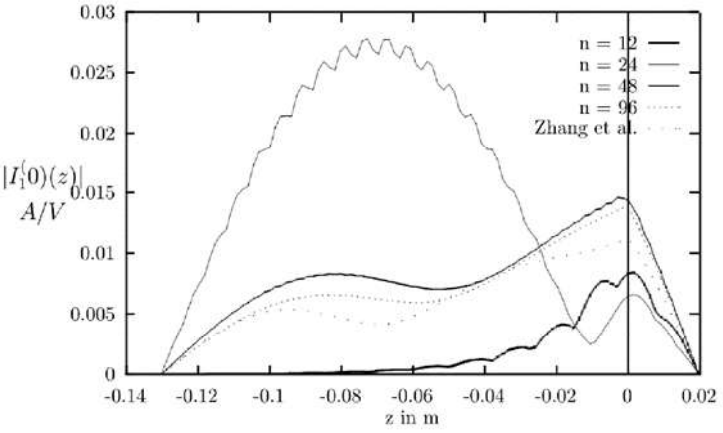

Fig. 4 displays the magnitude of the complex current distribution $|I_1^{(0)}(z)|$ for dipole 1, when the antennas of the array are excited with the voltages of the $m = 0$ phase sequence. The figure also includes the current distribution provided by Zhang's approximate model (Zhang *et al*, 1990), whose accuracy is experimentally verified. It is evident that as the number of basis functions N increases, the distributions obtained via the moment method soon converge and when that happens (for $N \geq 48$) they are in excellent agreement with the previously published curved.

FIGURE 5
MAGNITUDE OF THE TOTAL ELECTRIC FIELD$|E|$, ALONG THE Z AXIS OF THE ARRAY, WHEN ITS FOUR ELEMENTS ARE DRIVEN IN PHASE (ZERO PHASE SEQUENCE)

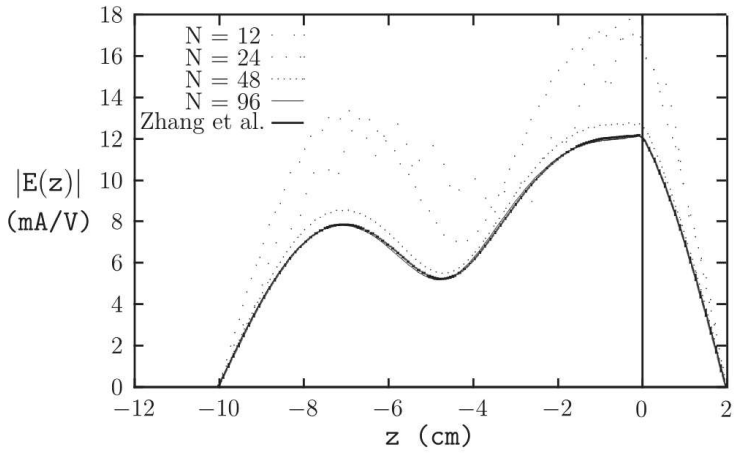

Fig. 5 illustrates the total electric field$|E|$, along the z axis of the array, when its four elements are driven in phase (zero phase sequence). Results from using various discretization densities are compared to each other, and to a field distribution computed with the application of Zhang's theory. Once convergence is established, any discrepancies existing between our approach for very coarse discretizations ($N = 12,24$) and that of Zhang, are minimized and become negligible. It must be pointed out that the results of

our method are obtained much more efficiently compared to the numerical complexity of Zhang's technique, as less arithmetic operations are involved in our implementation. However, we will not elaborate on this point as it is treated in detail in reference (Atlamazoglou *et al.,* 1998).

A quantity of primary interest in hyperthermia is the Specific Absorption Rate (SAR), as it is closely associated to the rate of temperature increase in a biological medium. SAR is defined as the spatial distribution of energy absorbed per unit mass, and it is measured in W/Kg. The SAR is a function of the electric field radiated by an interstitial antenna or array, and this relation is expressed in the form

$$SAR = \frac{1}{2}\frac{\sigma}{\rho}|E|^2 = \frac{\sigma}{2\rho}(|E_z|^2 + |E_r|^2) \tag{27}$$

where σ is the conductivity of the ambient medium (S/m), ρ is its density (kg/m^3), and $|E|$ the magnitude of the electric field (V/m).

FIGURE 6
NORMALIZED SAR PATTERN AT THE LATERAL PLANE OF THE ARRAY, FOR THE SYMMETRIC PHASE SEQUENCE

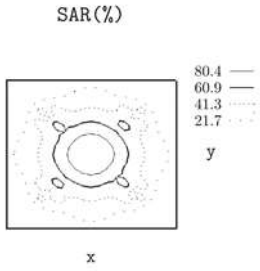

Fig. 6 displays the SAR pattern at the lateral plane ($z = 0$) of the array, for the symmetrical or zero phase sequence ($V_1 = V_2 = V_3 = V_4 = 1V$). The number of basis functions used is 48. The computation of SAR values takes place at distinct points over a 2 cm by 2 cm array on plane $z = 0$. These points are uniformly distributed over the surface, and the minimum distances between them are $\Delta x = \Delta y = 2mm$.

FIGURE 7
NORMALIZED SAR PATTERN AT THE AXIAL PLANE OF THE ARRAY, FOR THE SYMMETRIC PHASE SEQUENCE

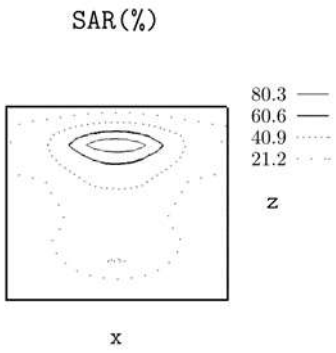

Fig. 7 illustrates the iso-SAR distribution at the axial plane of the array (the xz plane that is parallel to the antennas), again for the symmetric phase sequence and $N = 48$. The grid that we use for this SAR

computation has dimensions 4 cm by 14 cm, while its discretization steps are $\Delta x = 2mm$ and $\Delta z = 4mm$.

As Figs. 6 and 7 indicate, the deposition of energy exhibits a global maximum at the center of the array, while it is also especially high at the close vicinities around the antennas. The SAR pattern for zero phase sequence excitation, is non-uniform at both the lateral ($z=0$) and the axial ($y=0$) plane of the array.

At this point, it must be made clear that the SAR distributions computed are proportional to the rate of temperature increase for the tissue, only when that rate exceeds significantly the rate of temperature decrease due to heat conduction and blood perfusion. As a result of that, a steep gradient in SAR does not necessarily correspond to a steep temperature gradient, because of the smoothing effects of heat conduction and blood flow in living tissue.

The results of Figs. 6 and 7, indicate that the four-dipole circular array, with its element driven in phase, is able to heat an ellipsoidal region 2 cm in diameter and 6 cm long. This means that the array under study is suitable for heating small ellipsoidal tumors. In that case the dipoles must be placed at the periphery of the tumor to be heated, and oriented parallel to its major axis.

When the antennas 1 and 4 are driven in phase at 0^o, while 2 and 3 are driven in phase at 180^o, then the SAR patterns at the planes ($z=0$) and ($y=0$), have the forms shown at Figs. 8 and 9 respectively. The voltages of this excitation ($V_1=V_4=1$, $V_2=V_3=exp^{j\pi}$) do not belong in any of the four phase sequences of the array. However as we have shown in the previous section, the current distributions I_1,I_2,I_3 and I_4 can be expressed as functions of the phase sequence currents $I_i^{(m)}$.

FIGURE 8
NORMALIZED SAR PATTERN AT z = 0, WHEN $V_1=V_4=1$ AND $V_2=V_3=exp^{j\pi}$

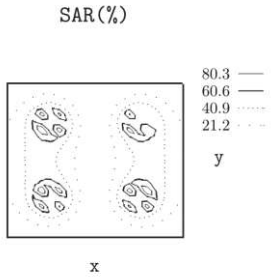

As it is expected, the non-symmetrical excitation of the dipoles has as a result the differentiation of the SAR pattern forms, compared to those of Figs. 6 and 7. The focal point, where the maximum energy deposition takes place, is not anymore at the center of the array. It is evident that its position depends on the phases of the excitation voltages of the antennas.

FIGURE 9
NORMALIZED SAR PATTERN AT y = 0, WHEN $V_1=V_4=1$ AND $V_2=V_3=exp^{j\pi}$

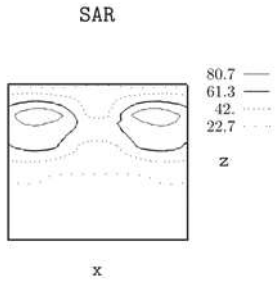

So, a suitable choice of these phases, can offer the ability to control the positioning of the focal point, as well as the overall form of the SAR pattern. A uniform SAR pattern is desirable for rising the temperature to a therapeutic level, while for maintaining it at that level more preferable is a SAR distribution with increased energy deposition at the periphery of the tumor, where heat conduction due to blood flow is higher.

In order to obtain a specific temperature distribution, the phases of the excitation voltages can be made to vary with time. This allows greater flexibility in energy deposition, and better control of the temperature distribution, that in clinical hyperthermia is of primary interest.

CONCLUSIONS

The method of moments for the analysis of an insulated dipole antenna embedded in a dissipative dielectric medium is extended for the study of interstitial antenna arrays used for microwave-induced hyperthermia. This solution of the coupled integral equation of the array is carried out with the method of symmetrical components. The insulating layers of the antennas are modeled by equivalent volume polarization currents, in a way that prevents the introduction of additional unknowns and numerical volume integrations.

Comparisons between our results and those obtained by well established techniques reveal excellent agreement for the current as well as the field distributions. This fact testifies to the validity and accuracy of our analysis, an accuracy that is achieved at a computational cost significantly lower to that of previous methods.

Furthermore, the analysis that we propose is more general than the existing ones, as it is not subject to the restriction that the complex permittivity of the ambient medium must be much greater than that of the dielectric coating. Our analysis does not even make the non-physical assumption that the insulating sheaths in which the dipoles are embedded, extend to infinity. On the contrary it can easily treat inhomogeneous coatings or partially coated antennas. Finally, the coupling between the dipoles that is usually neglected in the other approaches is taken fully into account in a simple and efficient manner.

REFERENCES

Atlamazoglou, P.E., & Uzunoglu N. K. (1998, July). A Galerkin moment method for the analysis of an insulated antenna in a dissipative dielectric medium. *IEEE Trans. Microwave Theory Tech.*, 46, 988-996.

Clibbon K. L., McCowen A., & Hand W.H. (1993, September). SAR distributions in interstitial microwave antenna arrays with a single dipole displacement. *IEEE Trans. Biomed. Eng.*, 40(9), 925-932.

Ebihara S. & Hashimoto Y. (2007). MoM Analysis of Dipole Antennas in Crosshole Borehole Radar and Field Experiments," *IEEE Transactions on Geoscience and Remote Sensing*, 45, 2435-2450.

Hahn G. M. (1982). *Hyperthermia and Cancer.* New York: Plenum, 1982, pp. 1-285.

Jacqmaer P., Geuzaine C., & Driesen J. (2008). Application of an electromagnetic modeling method for railway grounding systems subjected to lightining strikes. *th International Conference on Harmonics and Quality of Power 2008*, vol. ICHQP 2008, 1-6, 2008.

Jakobus J., Ruoss H., Geisbusch L., & Landstorfer F. M. (1999). Hybridisation of MoM and GMT for the numerical analysis of electromagnetic sources radiating in the vicinity of persons with implaned cardiac pacemakers. *Africon 1999 IEEE*, 2, 1041-1044.

King R. W. P., Trembly B. S., & Strohbhen J. W. (1983, July). The electromagnetic field of an insulated antenna in a conducting or dielectric medium. *IEEE Trans. Microwave Theory Tech.*, MTT-31(7), 574-583.

King R. W. P. (1990, September). The large circular array with one element driven. *IEEE Trans. Antennas Propagat.*, 38, 1462-1472.

Liu S., & Sato M. (2005). Transient radiation from an unloadede finite dipole antenna in a borehole: Expiremental and numerical results. *GEOPHYSICS*, 70, K43, 2005.

Mendecki J., *et al.* (1977). Microwave applicators for localized hyperthermia treatment of malignant tumors. *J. Bioeng,* 1, 511-518.

Mohsin S. A., Sheikh N. M., & Saeed U. (2008). MRI-induced heating of deep brain stimulation leads," *Physics in Medicine and Biology*, 53, 5745.

Mohsin S. A., Saeed U., Nyenhuis J., & Sheikh M. N. (2008, July). Scattering of the MRI field at 1.5T by a Vagus Nerve Stimulation Implant. *Antennas and Propagation Society International Symposium 2008*, AP-S 2008, IEEE, 1-4.

Park S. M., Kamondetdacha R., Amjad A., & Nyenhuis J. A. (2005). MRI safety: RF-induced heating near straight wires. *IEEE Trans.on Magnetics*, 41, 4197-4199.

Press W. H., Flannery B. P., Teukolsky S. A., & Vetterling W. T. (1989). *Numerical Recipes: The Art of Scientific Computing.* New York: Cambridge University Press, pp. 47-52.

Taylor L. S. (1978). Devices for microwave hyperthermia," in *Cancer Therapy by Hyperthemia and Radiation*, C. Streffer *et al.*, Eds., Baltimore, MD:Urban and Schwarzenberg, 1978, pp. 115-117.

Yeung C. J., Susil R.C., &. Atalar E. (2001). RF safety of wires in interventional MRI: using a safety index," *Engineering in Medicine and Biology Society 2001. Proceedings of the 23rd Annual International Conference of the IEEE*, 3, 2496-2498.

Yeung C. J., Susil R.C., &. Atalar E. (2002). RF heating due to conductive wires during MRI depends on the phase distribution of the tranmit field. *MAgnetic Resonance in Medicine*, 48, 1096, 2002.

Zhang Y., Dubal N. V., Takemoto-Hambleton R., & Joines W.T. (1988, October). The determination of the electromagnetic field and SAR pattern of an interstitial applicator in a dissipative dielectric medium. *IEEE Trans. Microwave Theory Tech.*, MTT-36(10), 1438-1443.

Zhang Y., Joines W. T., & Oleson J. R. (1990, February). Microwave hyperthermia induced by a phased interstitial antenna array. *IEEE Trans. Microwave Theory Tech.*, 38, 217-221.